



# Investigating the Release Mechanism of Calcein from eLiposomes at Higher Temperatures

Ghaleb A. Hussein<sup>1,\*</sup>, William G. Pitt<sup>2</sup>, Jacob B. Williams<sup>2</sup>, and Marjan Javadi<sup>2</sup>

<sup>1</sup>American University of Sharjah, Chemical Engineering Department EB1-230, AUS, Sharjah, United Arab Emirates

<sup>2</sup>Brigham Young University, Department of Chemical Engineering 350 CB, BYU, Provo, UT, 84604

Numerous nanocarriers are currently being investigated as drug delivery vehicles for transporting chemotherapeutics to cancer cells. Our research group has recently synthesized a new generation of echogenic liposomes based on the concept of encapsulating one or more nanoemulsion droplets inside a liposome (called an “eLiposome”). The concept is to use a nanoemulsion droplet with a low boiling point near body temperature, thus requiring only a small acoustic nudge to vaporize the droplet from liquid to gas and break open the eLiposome, thus releasing its contents. The purpose of this note is twofold. First, we wanted to show experimentally that eLiposomes remained stable at body temperature and retained their potential to deliver drugs through the ultrasonically-activated expansion of the emulsion nanodroplet. Additionally, we examined the physical mechanism potentially involved in the release of calcein at higher temperatures. Experimental results using calcein as a model drug confirmed the eLiposome stability at physiological temperatures and suggested that heterogeneous nucleation theory was capable of capturing the general release characteristics observed in this study. Heterogeneous nucleation of gas is possibly the main mechanism at play in passive release from eLiposomes at temperatures above body temperature. More research is needed to confirm the definitive physics of the model drug’s release from these novel nanovehicles.

**Keywords:** eLiposomes Stability, Calcein Release, Heterogeneous Nucleation, Fluorometry, Acoustic Droplet Vaporization (ADV).

## 1. INTRODUCTION

The first decade and a half of the 21st Century has seen a plethora of nanotechnology devices and concepts. This includes the field of medicine in which nanodevices have been employed in diagnostic and therapeutic applications.<sup>1–3</sup> Selective identification, precise delivery and successful repair are the hallmarks of useable nanotechnology in medicine. In the realm of drug delivery, nanodevices employ passive triggering and active triggering to deliver a therapeutic only at a designated site or tissue.<sup>4</sup> Passively triggered release is actuated by variances in the local environment, such as pH, temperature or redox state, which produce a change in the nanocarriers to release the sequestered therapeutic. Active release is triggered by some external action that can be focused on a particular site in the body, such as light, other electromagnetic fields, pressure waves (including ultrasound), or thermal heating. This report describes an ultrasonically-activated nanodevice that tightly sequesters drugs or nucleic acids and releases them only upon exposure to ultrasound (insonation).

Our lab has developed a nanodevice called an eLiposome (see Fig. 1) which consists of a nanosized liposome (a bilayer lipid shell enveloping an aqueous interior) containing the therapeutic and at least 1 nanodroplet of a perfluorocarbon liquid with a low boiling point.<sup>5–7</sup> The name “eLiposome” comes from *emulsion droplet* in a *liposome*. Release from an eLiposome is triggered by ultrasound via the phenomenon of acoustic droplet vaporization, in which ultrasonic pressure waves cause a liquid droplet to change phase to a gas bubble of much larger volume.<sup>8</sup> The expansion of the liquid emulsion droplet to a gas bubble causes the rupture of the liposomal membrane surrounding it, and thus releases the therapeutic payload upon insonation. We have demonstrated the controlled release of calcein (a model drug), doxorubicin (a chemotherapeutic) and DNA plasmids using eLiposomes and ultrasound of low power and low frequency.<sup>9</sup> We have used perfluoropentane (PFC5) and perfluorohexane (PFC6) as the emulsion nanodroplets in these eLiposomes. The former has a normal boiling point of 29 °C and the latter of 56 °C. They are both non-toxic and have very low solubility in water.

\*Author to whom correspondence should be addressed.

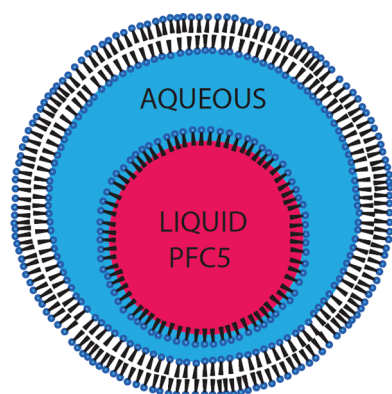


Fig. 1. Illustration of an eLiposome.

Given that the boiling point of PFC5 is below body temperature (37 °C), a question arises concerning the thermal stability of these eLiposomes. Prior studies have shown that small emulsion droplets of PFC5 do not boil at 37 °C.<sup>10–12</sup> This has been attributed to the Laplace pressure created by the highly curved interface of the nanosized droplet, which creates an internal droplet pressure greater than the vapour pressure of the PFC5 at 37 °C, so no boiling occurs.<sup>13</sup> However, no studies have been done on our eLiposome construct to determine the upper boundary of temperature above which the droplets are no longer stable, but will expand to gas. Furthermore, the chemical activity of the PFC5 inside the Laplace-pressurized droplet is higher than the activity outside the droplet, so there will be a small driving force for PFC5 to diffuse from inside the eLiposome to outside, thus eventually depleting the eLiposome of its rupture mechanism.

The purpose of this study was to show that the eLiposomes remained stable and retained their potential to deliver drug through the ultrasonically-activated expansion of the emulsion nanodroplet at body temperature. We also investigated the loss of drug delivery potential at temperatures above 37 °C. Our results show that eLiposomes with PFC5 droplets are stable at body temperature, but become unstable at higher temperatures.

## 2. MATERIALS AND METHODS

PFC5 nanoemulsions were made by placing 0.1 mL of cold (0 °C) perfluoropentane (PFC5) (b.p. = 29 °C) in a cold flask that was previously coated with a layer of dipalmitoylphosphatidylcholine (DPPC). The DPPC and PFC5 were sonicated on ice with a 20-kHz ultrasound probe for 1 min at 1 W/cm<sup>2</sup>. The resulting droplets had a diameter between 100 and 200 nm as measured by dynamic light scattering. They were subsequently extruded through a 100-nm filter to decrease their size and narrow the distribution.

In a separate flask, conventional liposomes were made by drying DPPC, cholesterol and DSPE-PEG (2000) amine (Avanti Polar Lipids) onto a glass flask and then hydrating

the resultant layer with buffer. The mixture was sonicated and extruded through a 200-nm filter to produce unilamellar liposomes of about 200 nm in diameter.

Calcein-filled eLiposomes were made by mixing 1 mL of 100-nm PFC5 emulsion droplets, 1 mL of 200-nm liposomes, and 2 mL of 30 mM calcein, and then sonicating the mixture on ice 3 times for 30 seconds with 60 seconds rest between each sonication. We believe that the sonication transiently breaks open liposomes, and the emulsion droplets and calcein enter the liposome membrane before it re-seals. External emulsion droplets (not captured inside the eLiposome) and empty liposomes were removed by centrifugation on a sucrose/glucose/NaCl density column with the resultant eLiposomes collecting between the sucrose and glucose layers.<sup>7</sup> CryoTEM imaging has shown emulsion droplets inside the liposomes.<sup>5,7</sup> The final calcein concentration in the eLiposomes was estimated to be 15 mM which was in the self-quenched region and thus had minimal fluorescence. As the calcein escaped from the carrier, its concentration was diluted to the linear fluorescence range (<20 μM) where the fluorescence is proportional to concentration. The fraction of calcein released was quantified as previously published.<sup>6</sup>

For these experiments 30 μL of the calcein loaded nanocarriers were mixed in 2 mL of PBS (pH = 7.4) in a cuvette. The excitation and emission wavelengths were set respectively at 488 and 520 nm, and the fluorescence emission continuously recorded. Figure 2 shows the fraction of calcein released from eLiposomes over a period of one hour. There is no insonation applied in these experiments, so we were measuring spontaneous release of calcein from quiescent eLiposomes.

## 3. RESULTS AND DISCUSSION

A rapid release of calcein from our eLiposomes was observed at 59 °C and 49 °C, but minimal release was observed at body temperature (37 °C) or room temperature (25 °C) as seen in Figure 2. The latter temperature is

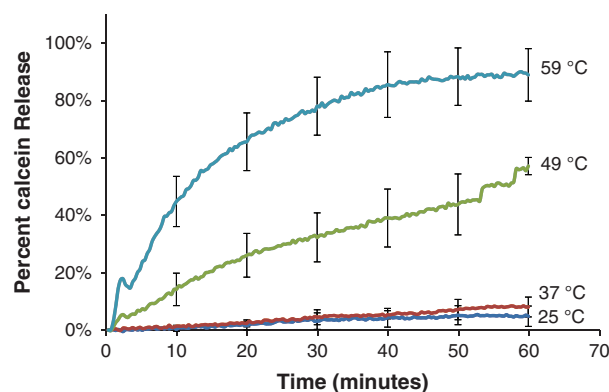


Fig. 2. Average fraction of calcein release from eLiposomes incubated, NOT insonated, at various temperatures. Error bars indicate the standard deviation of several experiments ( $n \geq 3$ ) at selected times.<sup>14</sup>

below the normal boiling point of PFC5 (29 °C), but the former temperature is significantly above the normal boiling point. The stability of the PFC5 emulsions above its normal boiling point is attributed to the Laplace pressure which increases the internal pressure inside the droplet such that the vapour pressure remains below the local (internal) pressure and no gas forms.<sup>12</sup> We postulate and discuss three possible causes for the rapid release observed at 49 °C and 59 °C, namely:

- (1) increasing temperature increases the passive diffusion of calcein across the liposomal bilayer
- (2) the phospholipids in the bilayer experience a membrane transition at its transition temperature
- (3) the liposome is ruptured by the formation of a gas bubble. Below, we test these postulates against the experimental evidence to reject or accept possible physical mechanisms at play in this drug delivery system.

For the first postulate we assume that the temperature dependence of the diffusivity of calcein through the lipid bilayer membrane can be modelled by an Arrhenius-type equation,

$$D = D_o \exp\left(\frac{-E_d}{RT}\right) \quad (1)$$

where  $D$  is the diffusivity coefficient,  $D_o$  is the pre-exponential constant,  $E_d$  is the activation energy for diffusion,  $R$  is the universal gas constant, and  $T$  is the absolute temperature. Initial release rates, which are proportional to  $D/D_o$ , were calculated and the negative of the natural logarithms of the release rates were plotted versus the inverse of absolute temperature. The data was then fit using a linear equation (see Fig. 3). Using the slope of the fitted line, the  $E_d$  (see Eq. (1)) was estimated to be 110 kJ/mol. However, this value seems to be uncommonly high for diffusion of organics through organics. Work done by Maherani et al.<sup>15</sup> who investigated the temperature dependency of the permeability of DPPC-liposomes to calcein provides data from which the activation energy for diffusion was calculated to be 51 kJ/mol. Although this activation energy is approximately 50% lower than what we deduced in our experiments, it is quite significant and thus casts doubt

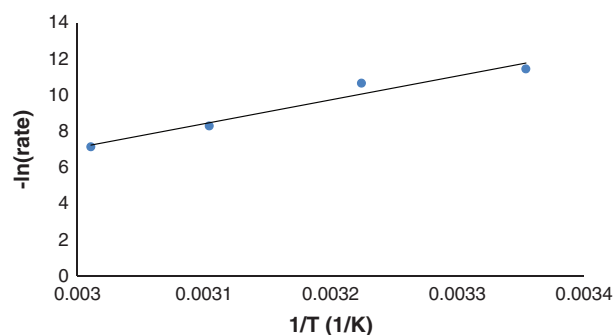


**Fig. 3.** Negative of the logarithms of the initial fractional calcein release rates versus inverse temperature. The line is a linear regression of the data points.

upon the first above mentioned hypothesis. To illustrate the significance of this difference, at 15 min of incubation, Maherani et al. reported just over 1% release of calcein at 50 °C, whereas in this work just over 20% release was observed at 49 °C after 15 min. This is 20-fold faster release than published data. Therefore, although the data apparently fits Eq. (1), the value of the activation energy is so high that it is unlikely that this is the sole mechanism of calcein release.

As for the second postulate, an increase in calcein release as a result of membrane transition would show a maximum at the transition temperature on a plot of rate versus temperature.<sup>16,17</sup> The membrane transition temperature for DPPC is 41 °C.<sup>15</sup> As seen in Figure 4, the data does not have a maximum release at the transition temperature that would be expected if release was solely based on membrane transition and if there were changes in membrane diffusivity as it changed from gel to liquid crystal states of the bilayer. The rate actually appears to increase exponentially as a function of temperature. Therefore it is also unlikely that the membrane transition of the phospholipids is the sole mechanism of calcein release.

The third postulate of gas bubble nucleation above the normal boiling point involves fairly complex theory. Firstly, the apparent boiling point of the PFC5 droplet increases due to the additional pressure imposed by the Laplace pressure ( $\Delta P_{Lp}$ ). The Laplace pressure is an additional pressure imposed on the interior of a sphere due to the curved interface, and is a function of the interfacial energy ( $\gamma$ ) and the radius ( $R$ ) of the emulsion droplet:

$$\Delta P_{Lp} = \frac{2\gamma}{R} \quad (2)$$

The total pressure of the emulsion droplet is the sum of atmospheric pressure ( $P_{atm}$ ), the hydrostatic pressure ( $P_{hyd}$ ), and the Laplace pressure. If gas nucleation sites are present, a gas bubble may form when the total pressure

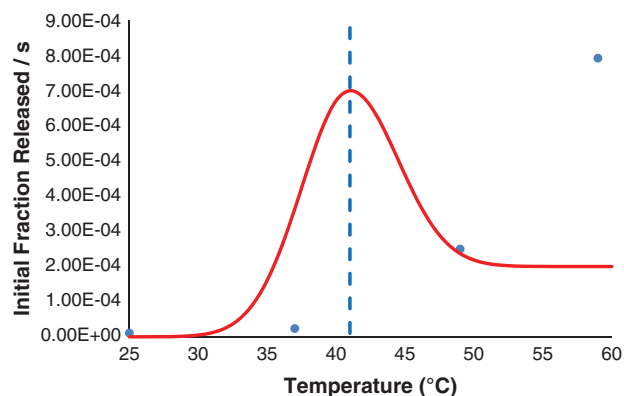


**Fig. 4.** Plot of initial fractional calcein release rates versus temperature. The dotted vertical line represents the literature value of the transition temperature for DPPC (41 °C). The solid line is a representation expected changes in membrane permeability<sup>16</sup> for passive transport across phospholipid bilayers.

inside the nanoemulsion (left side of Eq. (2)) drops below the local vapour pressure:

$$P_{\text{atm}} + P_{\text{hyd}} + \Delta P_{\text{Lp}} \leq P_{\text{vap}}(T) \quad (3)$$

Ignoring any hydrostatic pressure ( $\rho g \Delta h$ ), if one takes the interfacial energy of the phospholipid-coated PFC nanoemulsion to be 3.8 dyn/cm,<sup>18</sup> and a nanoemulsion with a diameter of 100 nm, the boiling point will increase from 29 °C to approximately 57 °C. If the droplet were 200 nm, the apparent boiling point would only be 45 °C. Emulsions for this study may range from 100 nm or lower to about 200 nm in diameter; therefore the first bubble could form once the temperature reached somewhere between 45 °C to 57 °C, with more bubbles likely to form as the temperature increases.

Nucleation must also occur in order for a gas phase to be formed. According to homogeneous nucleation theory the number of nucleation events occurring at a given temperature for a given unit volume per unit time can be approximated with the following equation:

$$J(T) = J_o \exp\left(\frac{-E_c}{kT}\right) \quad (4)$$

where  $J_o$  is a proportionality constant that has a weak dependence on temperature,  $E_c$  is the activation energy barrier for the formation of a nucleating cavity of a critical size,  $T$  is the absolute Temperature and  $k$  is Boltzmann's constant.<sup>19</sup> A derivation of  $J(T)$  is given below.<sup>20</sup>

For this study  $J_o$  is given by the following equation

$$J_o = N \left( \frac{2\gamma_g}{\pi m} \right)^{1/2} \quad (5)$$

where  $\gamma_g$  is the interfacial energy of the gas bubble with radius  $r^*$ ,  $N$  is the number density (molecules/m<sup>3</sup>) of liquid perfluoropentane (PFC5), and  $m$  is the molecular mass of PFC5.<sup>19</sup>

The interfacial energy is a function of temperature and was taken from the DIPPR database.<sup>21</sup> The dependence on temperature for  $J_o$  is weak compared to the terms inside of the exponent in Eq. (4).

There are two factors that contribute to the energy required ( $E$ ) to form a gas cavity within a liquid droplet:

- (1) surface energy of the cavity formed, and
- (2) free energy change during vaporization.

The surface energy of the nucleus formed is calculated as the interfacial energy of the gas bubble,  $\gamma_g$ , multiplied by its surface area,  $4\pi r^2$ , where  $r$  is the radius of the gas bubble. The free energy change during vaporization can be accounted for by the free energy of vaporization,  $\Delta G_v$ , of the entire vapour bubble:  $(4/3)\pi r^3 \Delta G_v$ . The energy required to form gas cavity with radius,  $r$ , is

$$E = \frac{4}{3}\pi r^3 \Delta G_v + 4\pi r^2 \gamma_g \quad (6)$$

The first term on the right hand side of Eq. (3) is negative at temperatures above the apparent boiling point of the PFC5 nanoemulsion, and is the driving force for nucleation. The second term on the right hand of the equation is always positive. The critical radius,  $r^*$ , is the radius of the bubble when  $E$  is at a maximum. Differentiating Eq. (3) with respect to  $r$  and setting it equal to zero provides a value for  $r^*$  (after rearranging):

$$r^* = \frac{-2\gamma_g}{\Delta G_v} \quad (7)$$

$\Delta G_v$  can be obtained using the following equation

$$\Delta G_v = \Delta H_v - T \Delta S_v \quad (8)$$

where  $\Delta H_v$  the latent is heat of vaporization, and  $\Delta S_v$  is the change in entropy during vaporization. For a pure liquid in equilibrium with its vapor phase at constant temperature and pressure, the free energy of the vapor phase is equal to the free energy of the liquid phase. Therefore, at equilibrium and the apparent boiling point,  $T_v$ ,

$$\Delta S_v = \frac{\Delta H_v}{T_v} \quad (9)$$

Assuming that  $\Delta S_v$  does not change much with temperature above the apparent boiling point, Eqs. (8) and (9) can be combined to yield,

$$\Delta G_v = \left( \frac{T_v - T}{T_v} \right) \Delta H_v \quad (10)$$

The latent heat of vaporization can be obtained from the Clapeyron Equation,

$$\frac{dP_v}{dT} = \frac{\Delta H_v}{T(V_v - V_L)} \quad (11)$$

where  $P_v$  is the corresponding pressure of the vapor phase in equilibrium with the liquid nanoemulsion droplet, and  $(V_v - V_L)$  is the change in volume accompanying the change from liquid ( $V_L$ ) to vapor phase ( $V_v$ ).  $V_L$  was assumed to be constant and was obtained from the DIPPR database. Assuming the vapor phase is an ideal gas,  $V_v$  can be written as

$$V_v = \left( \frac{R_g T}{P_v} \right) \quad (12)$$

where  $R_g$  is the universal gas constant. Assuming the  $P_v$  in Eq. (9) is constant and equivalent to the pressure inside the emulsion droplet, it can be defined as

$$P_v = P_{\text{atm}} + P_{\text{hyd}} + \Delta P_{\text{Lp}} \quad (13)$$

where  $P_{\text{atm}}$  is the atmospheric pressure,  $P_{\text{hyd}}$  is the hydrostatic pressure, and  $\Delta P_{\text{Lp}}$  is the Laplace pressure.  $P_{\text{hyd}}$  was neglected for this analysis, and  $\Delta P_{\text{Lp}}$  is defined as

$$\Delta P_{\text{Lp}} = \frac{-2\gamma_{\text{Lp}}}{R_{\text{em}}} \quad (14)$$

where  $\gamma_{Lp}$  is the interfacial energy of the nanoemulsion liquid and the phospholipids, and  $R_{em}$  is the radius of the PFC5 nanoemulsion droplet. The value of  $\gamma_{Lp}$  used in this analysis was  $3.8 \text{ dyne/cm}^2$ .<sup>17</sup>

The apparent boiling point,  $T_v$ , was determined by finding the temperature that corresponds to the  $P_v$  calculated in Eq. (13) and from an equation from DIPPR<sup>21</sup> for  $P_v$  as a function of  $T$ . This function was differentiated with respect to  $T$  and combined with Eqs. (11)–(14) to yield the following equation:

$$\Delta G_v = \left( \frac{T_v - T}{T_v} \right) T \left( \frac{R_g T}{2\gamma_{Lp}/R_{em}} - V_L \right) \frac{dP_v}{dT} \quad (15)$$

$\Delta G_v$  is a function of both the local temperature and the size of the nanoemulsion droplet. The  $r^*$  can now be calculated by inserting Eq. (15) into Eq. (7).  $E_c$  is defined as the activation energy at  $r^*$ , obtained by using  $r^*$  in Eq. (6).

For heterogeneous nucleation, the possible contaminants in the liquid phase provide a nucleation site and therefore reduce the energy required for nucleation. Depending on the mechanism, the energy required to create a nucleating gas phase is lowered. This is often attributed to a lower energy associated with forming the gas-liquid interface. To account for this reduction in surface energy required, we simply employed a scale factor,  $f$ , to the surface energy term to determine the  $E_c$  for heterogeneous nucleation. Equation (6) at the critical radius,  $r^*$ , then becomes

$$E_c = \frac{4}{3} \pi r^{*3} \Delta G_v + 4 \pi r^{*2} \gamma_g f \quad (16)$$

The value of  $f$  to fit the experimental data shown in Figure 6 was found to be  $f = 0.6678$ . It should be noted that this equation is only valid for temperatures above the apparent boiling point.

If we assume that the release rate of calcein is proportional to the number of nucleation events occurring, then the two events (nucleation and release) should follow the same trend. As seen in Figure 5, this is somewhat observed. The nucleation of gas bubbles begins about 10 K above the apparent boiling point. The nucleation rates increase exponentially at first and then continue to increase linearly. While the trends of homogeneous nucleation theory and the experimental data somewhat match, the experimental data begin to increase at an earlier temperature than homogeneous nucleation theory indicates. This suggests that there are emulsion droplets much larger than 200 nm, or that the theory is not sufficient. Therefore we turn to heterogeneous nucleation theory.

It is impossible to have homogeneous nucleation of a liquid at its equilibrium boiling point because the gas bubbles are unstable and will collapse spontaneously.<sup>20</sup> Therefore, nearly all experimentally formed gas bubbles are nucleated on surfaces of impurities in the system. Brennen<sup>19</sup> points out that the homogeneous nucleation is

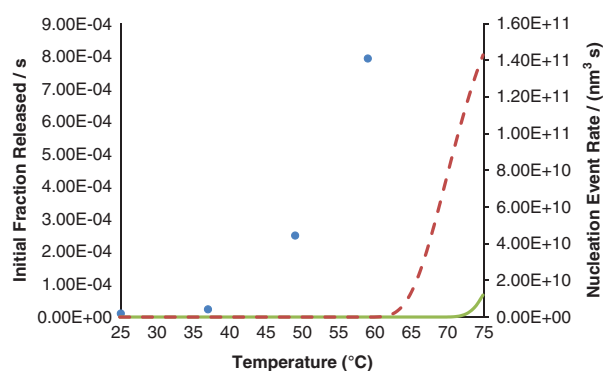


**Fig. 5.** Plot of initial fractional calcein release rates (left axis) and rate of nucleation events (right axis) versus temperature. The points indicate the experimental data and correspond to values on the left axis. The dotted line ( $d = 200 \text{ nm}$ ) and solid line ( $d = 100 \text{ nm}$ ) are theoretical homogeneous nucleation data and correspond to values on the right axis.

exceedingly difficult to obtain in the laboratory because even carefully distilled solvent still contains solid or dissolved chemical contaminants. The presence of contaminating particulates in the PFC5 emulsion would present sites for nucleation leading to heterogeneous nucleation. The activation energy for nucleation is lower for heterogeneous nucleation than for homogeneous nucleation, and therefore nucleation will happen at lower temperatures in heterogeneous nucleation. Using the same derivation for homogeneous nucleation, but using only a fraction of the interfacial energy of the nanoemulsion droplet it is possible to fit the trend in the data to the theory for nucleation at temperatures above the adjusted boiling point (Fig. 6).

The analysis presented above suggests that of the possible causes of calcein release from the liposomes containing nanosized PFC5 droplets, we can rule out some possibilities, and possibly accept others. The calcein release data does not fit what would be expected for temperature-induced changes in DPPC membrane permeability as heating caused a change from the solid-gel phase of the bilayer membrane to the liquid crystal phase. There is usually a

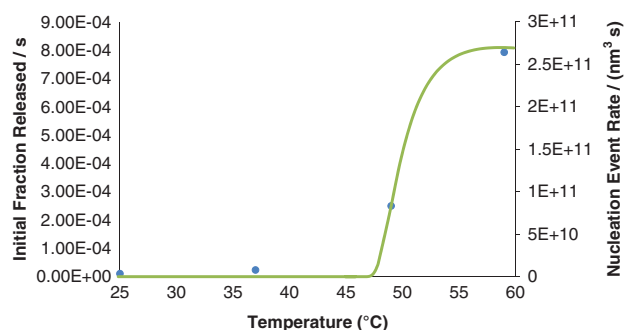


**Fig. 6.** Plot of initial fractional calcein release rates (left axis) and rate of nucleation events (right axis) versus temperature. The points indicate the experimental data and correspond to values on the left axis. The line ( $d = 200 \text{ nm}$ ) is heterogeneous nucleation theoretical data and corresponds to values on the right axis.

maximum in permeability right at the transition temperature, which would be 41 °C in this study. Thus we will dismiss this possibility as a major contributor, although this could possibly be happening in a small degree while other mechanisms dominate.

Likewise we can dismiss a thermal increase in diffusion of calcein through the DPPC bilayer. Diffusion ( $D$ ) is related to the membrane permeability ( $P$ ) through the solubility ( $k$ ) and membrane thickness ( $t$ ) by  $P = Dk/t$ . One would expect to see a maximum in  $D$  at the membrane transition temperature. The observation that the data fits an Arrhenius equation is probably fortuitous, and the very high activation energy also casts doubt on diffusion as a major mechanism for calcein release.

Homogeneous nucleation theory predicts that the release of calcein temperature would occur at higher temperatures than observed; and this rarely occurs except in highly purified and controlled experiments.

Heterogeneous nucleation theory was able to capture the general shape and trends observed experimentally, but definitive proof is lacking. Heterogeneous nucleation could be caused by a variety of sources, such as micelles of DPPC in the PFC5 droplets, solid contaminants in the PFC5 droplets, or even dissolved oxygen or nitrogen in the PFC5.

The purpose of our work is to first show experimentally that eLiposomes remained stable at body temperature thus upon injection into the patient these novel nanocarriers would not disintegrate and release their contents. Additionally, we examined the physical mechanism behind in the observed release of calcein from eLiposomes at elevated temperatures. Experimental results confirmed the nanovehicle's stability at physiological temperatures and suggested that heterogeneous nucleation theory was capable of capturing the general release characteristics observed in this study. Heterogeneous nucleation of gas is possibly the main mechanism at play in passive release from eLiposomes at temperatures above body temperature. More research is needed to confirm the definitive physics of the model drug's release from these novel nanovehicles.

Obviously, more research needs to be conducted to definitively answer this mechanistic question. However, the most important finding reported in this article is that the DPPC liposomes containing PFC5 emulsions are stable at body temperature (37 °C), even though this temperature is above the normal boiling point of PFC5 (29 °C).

These types of lipid vesicles may have potential for use in medicine as drug delivery vehicles.

**Acknowledgments:** The authors acknowledge the financial support of the Faculty Research Grant Type 1 (FRG1-2012), from the American University of Sharjah, Sharjah, United Arab Emirates.

## References and Notes

1. P. Mohan and N. Rapoport, *Molecular Pharmaceutics* 7, 1959 (2010).
2. A. T. Nguyen and S. P. Wrenn, *Wiley Interdiscip. Rev. Nanomed. Nanobiotechnol.* (2014).
3. Y. N. Xia, W. Y. Li, C. M. Cobley, J. Y. Chen, X. H. Xia, Q. Zhang, M. X. Yang, E. C. Cho, and P. K. Brown, *Accounts of Chemical Research* 44, 914 (2011).
4. G. A. Husseini and W. G. Pitt, *Advanced Drug Delivery Reviews* 60, 1137 (2008).
5. J. R. Lattin, D. M. Belnap, and W. G. Pitt, *Colloids Surf. B Biointerfaces* 89, 93 (2012).
6. J. R. Lattin, W. G. Pitt, D. M. Belnap, and G. A. Husseini, *Ultrasound Med. Biol.* 38, 2163 (2012).
7. M. Javadi, W. G. Pitt, D. M. Belnap, N. H. Tsosie, and J. M. Hartley, *Langmuir* 28, 14720 (2012).
8. C. Y. Lin, M. Javadi, D. M. Belnap, J. R. Barrow, and W. G. Pitt, *Nanomed. Nanotech., Biol. and Med.* 10, 67 (2014).
9. M. Javadi, W. G. Pitt, C. M. Tracy, J. R. Barrow, B. M. Willardson, J. M. Hartley, and N. H. Tsosie, *J. Controlled Release* 167, 92 (2013).
10. T. Giesecke and K. Hynynen, *Ultrasound in Medicine and Biology* 29, 1359 (2003).
11. N. Rapoport, Z. Gao, and A. Kennedy, *J. Natl. Cancer Inst.* 99, 1095 (2007).
12. P. S. Sheeran, S. Luois, P. A. Dayton, and T. O. Matsunaga, *Langmuir: The ACS Journal of Surfaces and Colloids* 27, 10412 (2011).
13. P. S. Sheeran, S. H. Luois, L. B. Mullin, T. O. Matsunaga, and P. A. Dayton, *Biomaterials* 33, 3262 (2012).
14. G. A. Husseini, W. G. Pitt, and J. Marjan, *Technology in Cancer Research and Treatment* (2014), in press.
15. B. Maherani, E. Arab-Tehrany, A. Kheirloomoom, D. Geny, and M. Linder, *Biochimie* 95, 2018 (2013).
16. W. V. Kraske and D. B. Mountcastle, *Biochim. Biophys. Acta* 1514, 159 (2001).
17. W. Stillwell, *An Introduction to Biological Membranes: From Bilayers to Rafts*, Academic Press, London (2013).
18. A. Kabalnov, J. Weers, R. Arlauskas, and T. Tarara, *Langmuir* 11, 2966 (1995).
19. C. E. Brennen, *Cavitation and Bubble Dynamics*, Oxford University Press (1995).
20. M. Blander and J. L. Katz, *AIChE Journal* 21, 833 (1975).
21. R. L. Rowley, W. V. Wilding, J. L. Oscarson, and N. F. Giles, *DIPPR* (2013).

Received: 13 November 2014. Accepted: 8 January 2015.